scientific reports

Check for updates

OPEN

Effects of the fatty acid synthase inhibitors triclosan and lapatinib on dengue virus and Zika virus infection

Suthatta Sornprasert[1], Janejira Jaratsittisin[1], Chanida Chumchanchira[1,2] & Duncan R. Smith[1]✉

Fatty acid synthase (FASN) has been shown to be critical in the replication of several viruses of the genus *Orthoflavivirus*. In this study the role two inhibitors of FASN that work through different mechanisms were investigated in dengue virus (DENV) and Zika virus (ZIKV) infections. Triclosan is a FASN inhibitor that targets the enol reductase domain of FASN, while lapatinib exerts an effect on FASN through acting on HER2, an upstream regulator of FASN. After determining cytotoxicity, a comprehensive analysis of the effect of these drugs in DENV 2 and ZIKV infection was undertaken. The results showed that triclosan had moderate antiviral activity against both DENV 2 (EC_{50} = 10.21 µM; Selective index (SI) = 3.99) and ZIKV (EC_{50} = 22.84 µM; SI = 5.49). Lapatinib had reasonable activity against DENV 2 (EC_{50} = 4.9 µM; SI = 26.09), but computer modeling suggested that lapatinib had the potential to be a directly acting antiviral by binding to NS5. The result of that analysis suggested that lapatinib was a better fit with ZIKV NS5 than DENV NS5, and this was confirmed as the EC_{50} for lapatinib towards ZIKV was was 2 µM and the calculated SI was 37.92. The results of triclosan are consistent with other studies that use inhibitors that target other domains of FASN, suggesting that simply targeting the enzymatic activity of FASN is insufficient for therapeutic drug development, but that lapatinib, or similar molecules may have real therapeutic potential.

Mosquito-borne viruses have been a significant healthcare problem in tropical and subtropical countries over the last several decade. The majority of the mosquito-transmitted viruses that cause disease in humans come from the recently renamed genus *Orthoflavivirus* (previously genus *Flavivirus*[1]) with the genus including dengue virus (DENV), Zika virus (ZIKV), Japanese encephalitis virus (JEV), West Nile virus (WNV), and yellow fever virus (YFV).

DENV a major mosquito-transmitted virus is mainly transmitted to humans by *Aedes spp*. mosquitoes, and it is endemic in approximately 100 tropical and subtropical countries around the world, and DENV is believed to cause some 390 million infections worldwide per year[2]. The speies *Orthoflavivirus denguei* (previously species *Dengue virus*) consists of four viruses, categorized as DENV 1, 2, 3 and 4.

The majority of infections with DENV are believed to be asymptomatic[2], but infection can results in mild symptoms including fever, headache, rash, muscle pain and fatigue[3]. Infection produces a robust immune response giving extended, if not lifelong protection against the infecting virus[4]. However, heterotypic antibodies from a primary infection do not provide protection against a second infection with a different DENV. However these existing antibodies can potentiate the disease pathology through a process termed antibody dependent enhancement (ADE)[5]. Approximately 60% of symptomatic dengue patients are a consequence of secondary infections, and these patients are at greater risk of developing the more severe symptoms associated with dengue hemorrhagic fever (DHF) and dengue shock syndrome (DSS)[6].

The closely related *Orthoflavivirus* species *Orthoflavivirus zikaense* (previously species *Zika virus*), consists of one viral species composed of two[7]or three[8]lineages, with the first study identifying African and Asian lineages, while the latter study identified two distinct African lineages. During the past decade,

[1]Institute of Molecular Biosciences, Center for Advanced Therapeutics, Mahidol University, Nakhon Pathom 73170, Thailand. [2]Phd Degree Program in Biology, Faculty of Science, Chiang Mai University, Chiang Mai 50200, Thailand. ✉email: duncan_r_smith@hotmail.com

ZIKV has caused outbreaks in many countries around the world. The first significant outbreak occurred in French Polynesia as a consequence of the Asian lineage ZIKV, and ZIKV subsequently caused a very large outbreak in Brazil in 2015[9,10]. Most ZIKV-infected patients experience an asymptomatic infection, but approximately 20% of patients experience symptoms similar to those of DENV infection, including a low-grade fever, rash, and conjunctivitis[11]. However, the complications of ZIKV can be consequential, including Guillain-Barre syndrome[12]and fetal microcephaly. ZIKV can pass across the placenta of a pregnant woman and infect the fetus, especially in the first trimester period, damaging the fetus's brain development and causing congenital microcephaly as well as other abnormalities that are collectively called congenital Zika syndrome[13]. Currently, for both viruses (DENV and ZIKV) there are no effective drug for treatment of infection, and therapeutic intervention is mainly supportive treatment based on the symptoms.

Both DENV and ZIKV modulate the host cell machinery including the unfolded protein response[14,15], autophagy[16,17]and lipid metabolism[18,19]to facilitate viral replication. Lipid metabolism is essential for Orthoflaviviruses since lipids are involved in viral entry, fusion of nucleocapsid and release, viral replication, virion assembly, and budding[20]. The rate limiting enzyme in lipogenesis is fatty acid synthase (FASN)[21]. Human FASN is a homodimeric, multi-domain enzyme of 272 kDa that contains seven catalytic domains, namely the β-ketoacyl synthase (KS) domain, an acyl carrier protein (ACP) domain, a β-ketoacyl reductase (KR) domain, an enol reductase (ER) domain, a dehydrase (DH) domain, malonyl/acyltransferase (MAT) domain and a thioesterase (TE) domain which collectively are responsible for converting malonyl CoA and acetyl-CoA into the endproduct, palmitate, which is the substrate for synthesizing long chain fatty acids[22]. Studies have shown that targeting FASN can have a significant effect on Orthoflavivirus replication. SiRNA mediated knock-down of FASN has been shown to significantly affect DENV replication[23], and the drug orlistat which targets the TE domain of FASN has been shown to inhbit DENV, ZIKV and JEV replication[24]. FASN is known to be upregulated in cells infected with ZIKV and WNV[25,26], and additionally studies in DENV have shown that it can be relocalized to the replication complex[27]. Other drugs including cerulenin, C75, EGCG, and flavonoids are known to target FASN and to inhibit viral replication, but as of today none of them are clinically available for treatment in cases of Orthoflavivirus infection[28].

Given the impact and importance of FASN in supporting Orthoflavivirus replication, we investigated the possible antiviral activity of two drugs, one of which, triclosan, targets FASN directly and has been shown to inhibit the activity of FASN in the MCF-7 and SKBr-3 cell lines[29], while the second, laptanib indirectly targets FASN by inhibiting phosphorylation of HER2, which subsequently inhibits FASN phosphorylation and FASN function[30].

Materials and methods

Cell lines and viruses

The human embryonic kidney cell line HEK293T/17 (ATCC CRL-11268), the hepatocellular carcinoma liver cell line HepG2 (ATCC HB-8065), the hepatocyte-derived carcinoma cell line Huh7[31], the human lung adenocarcinoma cell line A549 (ATCC CCL-185), the Lilly Laboratories Cell Monkey kidney 2 line LLC-MK2 (ATCC CCL-7) and the African green monkey kidney cell line Vero (ATCC CCL-81) were grown in Dulbecco's Modified Eagle's Medium (DMEM, GIBCO, Invitrogen, Grand Island, NY) supplement with either 10% Fetal Bovine Serum (FBS, GIBCO, Invitrogen, Grand Island, NY) or 5% FBS (for LLC-MK2 and Vero). The mosquito cell line, C6/36 (ATCC CR-1660), was grown in Minimal Essential Medium (MEM, GIBCO, Invitrogen, Grand Island, NY) supplemented with 5% FBS. FBS was heat-inactivated at 56 °C for 30 min before use. All cell lines were cultured at 5% CO_2, 37 °C, except for C6/36 which was incubated at 28 °C without CO_2 supplementation. DENV 2 (strain 16681; NCBI Accession number NC_001474) was propagated in the C6/36 cells, and supernatants containing viral particles were harvested at 5 days post-infection and kept at −80°C until used. ZIKV (Asian lineage SV0010/15; NCBI accession number. KX051562.1) was kindly provided by the Armed Forces Research Institute of Medical Science (AFRIMS), Thailand, and ZIKV-MU1-2017 (identical to NCBI Accession number MF996804) was isolated from a case of congenital Zika syndrome as previously reported[32]. The stock of each ZIKV strain was propagated in the C6/36 cells. Supernatants that contained viral particles were harvested once cytopathic effects appeared and were kept at −80°C until used. All virus stocks were confirmed by commercial Sanger DNA sequencing (Macrogen, Seoul, Korea) and quantitated for viral titer by plaque assay exactly as previously described[24].

Toxicity assays

Triclosan, orlistat (Merck KGaA, Darmstadt, Germany), lapatinib (Abcam, Cambridge, UK), and the mitogen-activated protein kinase (MEK) inhibitor, U0126 (Cell Signaling Technology, Danvers, MA) were dissolved in dimethyl sulfoxide (DMSO) (Merck KGaA) to obtain final stock concentrations of 100 mM for triclosan, 50 mM for lapatinib, 10 mM for U0126, and 38.5 mM for orlistat. All compounds were stored at −20 °C except orlistat which was stored at 4 °C until used. The toxicity was analyzed by observing cell morphology, trypan blue exclusion assays, and MTT assays. Cell morphology and trypan blue counts were undertaken by seeding HEK293T/17 or A549 cells at 5×10^5 cell/well in 6-wells plate, and subsequently treated with different drug concentrations in normal culture medium at 5% CO_2, 37 °C for 24 h. Cell morphology was observed at 10x magnification by an inverted microscope and images were

captured by NIS-Elements Analysis software. After 24 h, the treated cells were dissociated into a single cell suspension using trypsin, and 0.4% trypan Blue was added at a dilution of 1:1. Cells were counted in a hemocytometer under an inverted microscope and the percentage living cells was determined. MTT assays on the compound were undertaken in HEK293T/17 and A549 cells using the MTT (Thiazolyl Blue Tetrazolium Bromide (MTT); A2231, PanReac AppliChem, Darmstadt, Germany) as recommended by the manufacturer at 24 h post-treatment. Compound CC_{50} values were calculated using the freeware ED50plus v1.0 software (http://sciencegateway.org/protocols/cellbio/drug/data/ed50v10.xls). All experiments were taken independently in triplicate. The average of each replicate was used to plot non-linear regression plots to calculate CC_{50} and EC_{50}.

Virucidal assays

The compounds together with a negative control (culture medium or DMSO) were incubated directly with a known viral titer of DENV 2 or ZIKV at 37 °C, 5% CO_2 for 1 h. Viral titer was subsequently undertaken by standard plaque assay exactly as described previously[33]. All samples were analyzed independently in triplicate, with duplicate plaque assay.

Activity of triclosan against DENV 2 infection

Evaluation of the activity of triclosan was undertaken with a combination of pre- and post-infection treatment essentially as previously described in the evaluation of orlistat as an antiviral agent[24]. Briefly, HEK293T/17 cells were grown in 6-well plates (plated at a density of 5×10^5 cells/well) under standard conditions overnight. The medium was removed and replaced with fresh growth medium containing triclosan or the positive control, orlistat, after which the plates were incubated at 37 °C, 5% CO_2 for 1 h. Following that cells were infected with DENV 2 at a multiplicity of infection (MOI) of 5 and cells were at 37 °C, 5% CO_2 for 2 h. The inoculating titer medium was removed and replaced with triclosan or orlistat (as appropriate) diluted in growth medium. The plates were incubated at 37 °C, 5% CO_2 for 36 h before cells and supernatant were collected. All experiments were conducted independently in triplicate.

Antiviral activity of lapatinib against DENV 2 and ZIKV infection

HEK293T/17 or A549 cells were seeded in 6-well plates (at a density of 5×10^5 cells/well) and were incubated in growth media for 24 h. Cells were infected with DENV 2 at MOI 5, or with ZIKV at MOI 1 and cells were incubated at 37 °C, 5% CO_2 for 2 h. After that, the viruses were removed, then lapatinib or U0126 diluted in growth medium was added and the plates were incubated at 37 °C, 5% CO_2 before cells and supernatant were collected at the appropriate time point. All experiments were undertaken independently in triplicate.

Flow cytometry analysis

To deteremine the level of infection cells were dissociated from the plate by trypsinization. Single suspension cells were washed with 1X PBS and blocked using 10% normal goat serum on ice for 30 min. Subsequently, cells were washed with 1% bovine serum albumin (BSA) (Capricorn Scientific, Germany) in 1X PBS and then fixed with 4% paraformaldehyde in 1X PBS for 20 min in the dark. After that cells were washed with 1X PBS and permeabilized with 0.2% Triton X-100 (Merck, Burlington, MA) for 10 min in the dark. Cells were then washed and incubated with primary antibodies, either a pan-specific mouse monoclonal anti-dengue E protein antibody HB114[34]at a 1:150 dilution, or a pan-specific mouse monoclonal anti-flavivirus antibody HB112[34] at a 1:3 dilution, for DENV 2 and ZIKV, respectively, at 4 °C, overnight. After that cells were washed three times with 1% BSA in 1X PBS and then incubated with a FITC conjugated goat anti-mouse IgG antibody (1:40) (KPL, Gaithersburg, MD) at room temperature, for 1 h in the dark. Then, the cells were washed as described before and resuspended in 1X PBS. Stained cells were measured by flow cytometery on a BD FACSymphony™ A1 Cell Analyzer BD Biosciences, Franklin Lakes, NJ), and analyzed by FLOWJO Single Cell Analysis Software version 10 (BD Biosciences, San Jose, CA). Each sample was analysed as three independent biological replicates.

Quantitation of DENV 2 and ZIKV RNA genome copy number

Real-time RT PCR was used to quantitate free viral RNA copy number of DENV 2 or ZIKV in the supernatant of infected cells. Briefly, an equal amount of supernatant was extracted using TRIzol™ reagent (Thermo Fisher, Waltham, MA) as recommended by the manufacturer. The extracted RNA was reverse transcribed to cDNA using RevertAid; (Thermo Fisher, Waltham, MA). Briefly, the RNA template was mixed with random hexamer primers, heated at 95°C for 2 min, and chilled on ice for 5 min. Then, the second mixture which contained 5X reaction buffer, Thermo Scientific™ RiboLock RNase Inhibitor, dNTP Mix, and ReverseAid Reverse Transcriptase was added to the first mixture and PCR undertaken under the following conditions; 42°C for 90 min, and 70°C for 10 min. The synthesized cDNA was diluted with DNase/RNase-free water before performing Quantitative Real-time PCR (qRT-PCR). cDNA template, NS1-F (5'-CAATATGCTGAAACGCGAGAGAAA-3') and NS1-R (5'-CCCCATCTATTCAGAATCCCT GCT-3') primers for DENV or ZIKE-RT-Fw2 (5'-TTGGAGGAATGTCCTGGTTCTCAC-3') and ZIKE-RT-RV2 (5'-AGTCAGGATGGTACTTGTACC-3') primers for ZIKV, and KAPA SYBR FAST qPCR Kit 2X Master MIX (Kapa Biosystems Inc, Woburn, MA) and qRT-PCR was undertaken using a Master cycle

ep real-plex real-time PCR machine (Eppendorf, Hamburg, Germany) under the following condition; 95 °C for 30 min and 40 cycles of 95 °C for 10 s, 60 °C for 30 s, and 72 °C for 20 s. The results were quantitated with a standard curve which was constructed by a known copy number of 10-fold serially diluted NS1 DENV or ENV ZIKV DNA fragments (10^0–10^8 copies).

Protein extraction and Western blot analysis

Treated and untreated cells were collected by scraping from 6-well plates and washed with 1X PBS. The cells were lysed using RIPA buffer supplement with 1X PIC (100X Protease inhibitor cocktail, Biobasic Inc, Ontario, Canada) and 1X PhosSTOP (Roche, Mannheim, Germany) for detection of phosphoproteins. An equal amount of protein was mixed with 5X SDS sample buffer and 0.1 M of dithiothreitol (DTT) and samples were heated at 100 °C for 5 min. Proteins were separated by 10% sodium dodecyl sulfate-polyacrylamide gel (SDS-PAGE) and transferred into nitrocellulose membranes (Whatman plc., Maidstone, United Kingdom) by wet-blot electrophoresis transfer (Bio-rad Laboratories, Richmond, CA) at a constant amplitude (300 mA) for 3 h. Then, membranes were blocked with 5% skim milk in TBS-T (Tris-buffer saline plus 0.05% Tween 20) or 5% BSA (for detecting phosphoproteins) at room temperature for at least 30 min with agitation. Membranes were incubated with primary antibodies to NS5-DENV (dilution 1:5000; MA517295, Thermo Fisher Scientific), ENV-DENV (dilution 1:5000; MA1-27093, Thermo Fisher Scientific), NS5-ZIKV (dilution 1:5000; GTX133312, GeneTex), ENV-ZIKV (dilution 1:5000; GTX133314, GeneTex), p-ERK (dilution 1:20000; 9101, Cell Signaling), ERK (dilution 1:20000; 9102, Cell Signaling), p-AKT (dilution 1:20000; 4060, Cell Signaling), AKT (dilution 1:20000; 9272, Cell Signaling), FASN (dilution 1:5000; sc-32233, SantaCruz), and GAPDH (dilution 1:10000; sc-55580, SantaCruz) at 4 °C, overnight. Membranes were washed with TBS-T, and then incubated with an appropriate secondary antibody including a horseradish peroxidase (HRP) conjugated rabbit anti-mouse IgG (dilution 1:5000; A9044, Merck KGaA) or a HRP-conjugated goat anti-rabbit IgG (dilution 1:5000; 31460, Pierce, Rockford, IL) at room temperature for 1 h with gentle agitation. Then, the membranes were washed and the signals were developed by using Immobilon Forte Western blot HRP Substrate (Merck KGaA, Darmstadt, Germany) and detected by X-ray film. All experiments were undertaken independently in triplicate.

Molecular Docking

Ligands and receptors Preparation

The structures of the full-length NS5 of ZIKV and DENV 2 were obtained from Protein Data Bank (PDB)[35,36], PDB code, 6LD3, and 5K5M, respectively. UCSF Chimera (version 1.17.3, https://www.cgl.ucsf.edu/chimera/download.html) was used for protein and ligand preparation and visualization Docking results were represented by the BIOVIA Discovery Studio software (https://www.3ds.com/products/biovia/discovery-studio). Non-amino acid residues and water were removed from the crystal structures of both proteins before docking. The preparation was done by first adding hydrogens for intermolecular interaction with the default method while docking. Then, the charges were assigned by Gasteiger charges. The ligand SDF files of lapatinib and the compound G8O were downloaded from the PubChem database (https://pubchem.ncbi.nlm.nih.gov/).

Docking

AutoDock Vina (version 1.1.2, https://vina.scripps.edu/) was used for docking the prepared proteins and ligands. To control the parameter of docking, the receptor search column options were equally set up for the volume of the box size ($25 \times 25 \times 25$ A°) and covered the samebinding site among the two NS5 protein. The receptor and ligand options were set at the default values provided by the program. The maximum number of binding modes, exhaustiveness of the global search, and the maximum energy difference between modes were set as the maximum values which were 10, 8, and 3 kcal/mol, respectively. The models which provided the lowest entropy were chosen as the representative of each viral species NS5.

Statistical analysis

The differences between treated and untreated conditions were determined by the unpaired student's T-test, GraphPad Prism version 8 for Windows (GraphPad Prism, La Jolla, CA, https://www.graphpad.com/). The data are represented as mean ± the standard error of the mean (SEM). The statistically significant difference threshold was represented by p-value (two-tailed) with the degree of significance showing as an asterisk; NS (non-significant, $P > 0.05$), * ($P \leq 0.05$), ** ($P \leq 0.01$), and *** ($P \leq 0.001$).

Results

The determination of DENV 2 infection in different human cell line

To optimize the infection of DENV 2 in a human cell line, three human cell lines namely HEK293T/17 cell, HepG2 cell, and Huh.7 were chosen for investigation. These cells were infected with DENV 2 at MOI 1, 2, and 5 and at 24 h post-infection the percentage infection was determined by flow cytometry. The results (Supplemental Fig. 1) showed that all three cells lines were permissive to DENV infection and that the highest level of infection was seen in HEK293T/17 at all MOIs investigated. This cell line was therefore selected for use in subsequent experiments.

The cytotoxicity of triclosan, orlistat, lapatinib and U0126

To determine the optimal concentration of the compounds under investigation (triclosan, lapatinib and U0126) HEK293T/17 cells were treated with the compounds at concentrations of 1, 5, 10, 20, 50, 100, and 200 µM. The cytotoxicity of all compounds was determined by evaluation of cell morphology, trypan blue exclusion assays, and MTT assays. Cell morphology changes were observed at a concentration of 20 µM triclosan (Supplemental Fig. 2A) and at 100 µM lapatinib and U0126 (Supplemental Fig. 2B and 2C top panels, respectively). The compounds under investigation had been solubilized in DMSO, and therefore cells were treated with an equal amount of the final DMSO concentration as a control (Supplemental Fig. 2B, C, lower panels). The cell morphology of HEK293T/17 treated with 1% DMSO was markedly changed (Supplemental Fig. 2C, lower panel), suggesting that the morphology change seen in the cells when treated with 100 µM U0126 (Supplemental Fig. 2C, top panel) resulted directly from the DMSO. Positive and negative cell controls for morphological changes were milliQ water (100%) and DMEM. (Supplemental Fig. 2D).

For both the trypan blue exclusion assay and the MTT assay, a concentration of triclosan at or above 20 µM showed a significant loss of cell viability as compared to the DMSO control (Fig. 1A, D). A significant reduction of cell viability was seen at 50 µM for lapatinib (Fig. 1B, E) and at 200 µM for U0126 (Fig. 1C) in the trypan blue exclusion assay, while the MTT assays showed significant loss of viability at 50 µM (Fig. 1F).

The CC_{50}(cytotoxic concentration 50%) values were calculated from the MTT assays and were 40.74 µM, 127.86 µM and 195.12 µM for triclosan, lapatinib and U0126 respectively. Thus, from all three experiments concentrations of 10 µM were used for triclosan and U0126, while 20 µM was selected for lapatinib. In addition, the well characterized FASN inhibitor orlistat was used as a positive control at concentrations of 10 and 20 µM based on our earlier studies[23,24].

Antiviral activity of triclosan against DENV 2

To determine for antiviral activity of triclosan, which acts directly on the enoyl reductase domain, the condition for treating the cells was set as a combined pre- and post-treatment as used in our earlier study on orlistat[24]. HEK293T/17 cells were therefore pre-treated with the maximum concentration of the compounds that did not show signs of significant toxicity to the cells. Cells were therefore incubated with 5 and 10 µM triclosan and 10 and 20 µM orlistat for 1 h, after which the medium was removed and cells were then infected with DENV at MOI 5 for 2 h after which the inoculating media was removed and replaced with normal medium containing the appropriate compound and cells were then incubated for 36 h. The antiviral activity was evaluated in both cells and supernatants including the percentage of infection, viral production, viral genome copy number, and viral protein expression. HEK293T/17 cell morphology was not changed by either DENV 2 infection or treatment with both compounds (Fig. 2A.) We additionally evaluated whether the compounds had a direct virucidal activity by incubating the compounds directly with stock DENV 2 for one hour, after which the titer was established. There was

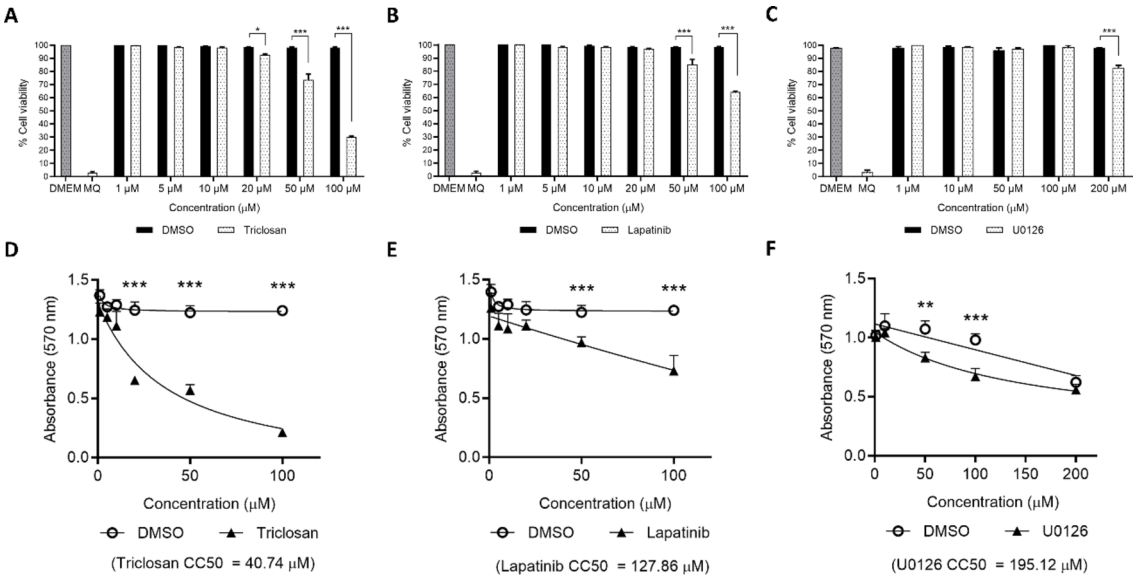

Fig. 1. Cytotoxicity assays. HEK293T/17 cells were treated with different concentrations of triclosan, lapatinib and U0126 for 24 h after the toxicity of the compounds was determined by trypan blue exclusion assay (**A**-**C**), and MTT asays (**D**-**F**). All experiments were taken independently in triplicate. $^{*}P<0.05$, $^{**}P<0.01$, $^{***}P<0.001$.

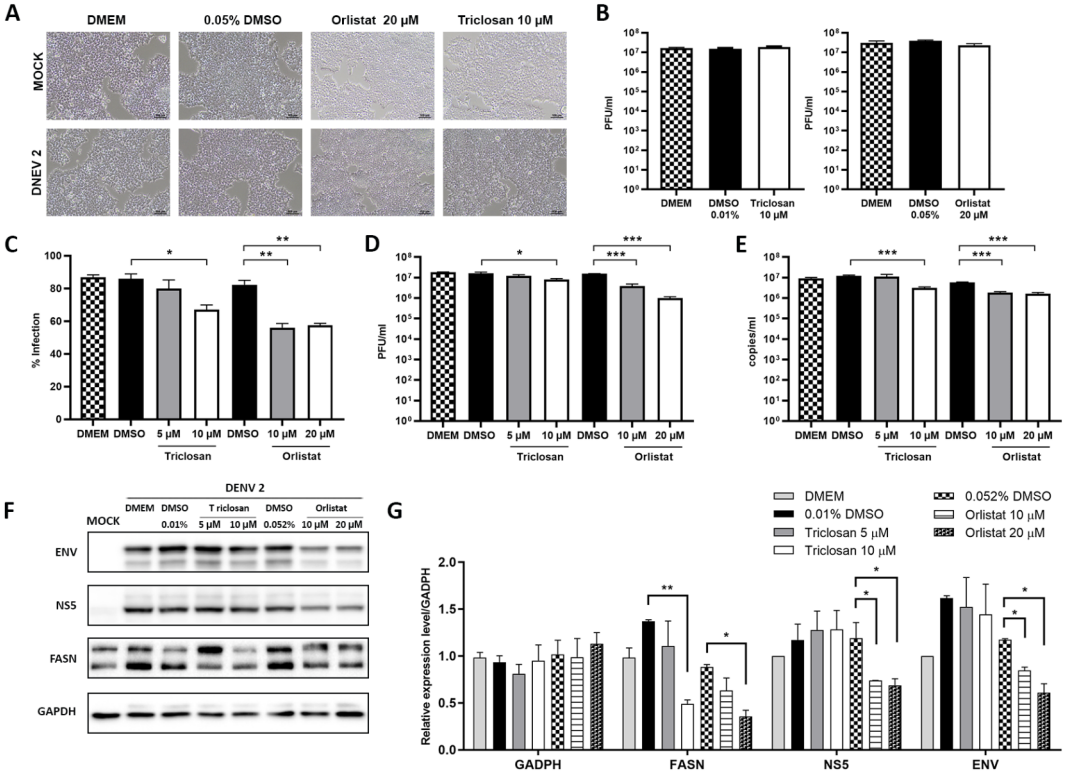

Fig. 2. Antiviral activity of triclosan against DENV 2. Triclosan and orlistat were used to pre-treat, and then post-treat HEK29T/17 cells after DENV 2 infection at MOI 5. The cells were collected at 36 h post-infection investigated for the (**A**) cell morphology (**B**) virucidal activity (**C**) percentage of infection (**D**) viral production (**E**) viral genome copy (**F**) viral protein expression. Quantitation of western blots shown in (**F**) is given in panel (**G**) with normalization against GAPDH. All experiments were conducted as independent triplicates, with duplicate plaque assay where appropriate. $^{*}P<0.05$, $^{**}P<0.01$, $^{***}P<0.001$. Composite images are shown (**F**) consisting of successive antibody probings of the same membrane which are separated by white bars. Full, uncropped western blots can be found in the supplemental materials.

no apparent direct virucidal activity of either compound (Fig. 2B). Both compounds at a concentration of 10 μM showed a significant reduction of the percentage of DENV 2 infection (Fig. 2C) and viral titer (Fig. 2D) and viral genome copy number in the supernatant (Fig. 2E). A concentration of triclosan lower than 10 μM could not inhibit viral infection and production (Fig. 2C-E). While both orlistat and triclosan at 10 μM can reduce FASN expression in the treated cells (Fig. 2F, G), a reduction in the expression of E and NS5 proteins was only observed with orlistat (Fig. 2F and G). The effective concentration that showed a 50% reduction in virus production (EC_{50}) was approximately 10.21 μM. The selective index (SI) of triclosan for treatment of DENV 2 infection is therefore 3.99.

To initially determine the antiviral activity of triclosan against another Orthoflavivirus, the antiviral activity against ZIKV was determined. The cytotoxicity of triclosan was determined by treating A549 cells with different concentrations (1, 10, 50, 100, and 200 μM) of triclosan for 24 h and cytotoxicity was evaluated by an MTT assay. The CC_{50} of triclosan was 125.51 μM (Supplemental Fig. 3). A594 cells were therefore infected with ZIKV and the infected cells were then treated with triclosan at concentrations of 20, 30, 40 and 50 μM for 24 h, after which virus production was determined by plaque assay. The results showed that post-treatment with triclosan of at least 40 μM reduced the viral production from ZIKV-infected cells. (Supplemental Fig. 4), and the calculated EC_{50} was 22.84 μM, giving an SI of 5.49.

Antiviral activity of lapatinib against DENV 2

To investigate the antiviral activity of lapatinib, HEK293T/17 cells were infected with DENV 2 at MOI 5, and cells were post-iinfection treated with 10 μM lapatinib or 10 μM U0126 for 24 h. The antiviral activity of both inhibitors was evaluated in both the cell and supernatant by measuring the percentage of viral infection, the viral production, viral genome copy number, and viral protein expression. The cell morphology of HEK293T/17 cells was not changed by either DENV 2 infection or treatment with lapatinib or U0126 (Fig. 3A). Neither drug had virucidal activity against DENV 2 which showed no significant difference when the virus was incubated directly with the drugs compared with the media only or the drug diluent (DMSO) (Fig. 3B). Lapatinib at a concentration of 10 μM significantly reduced the percentage of virus infection, viral production, and viral genome copy number (Fig. 3C-E). Interestingly, treatment

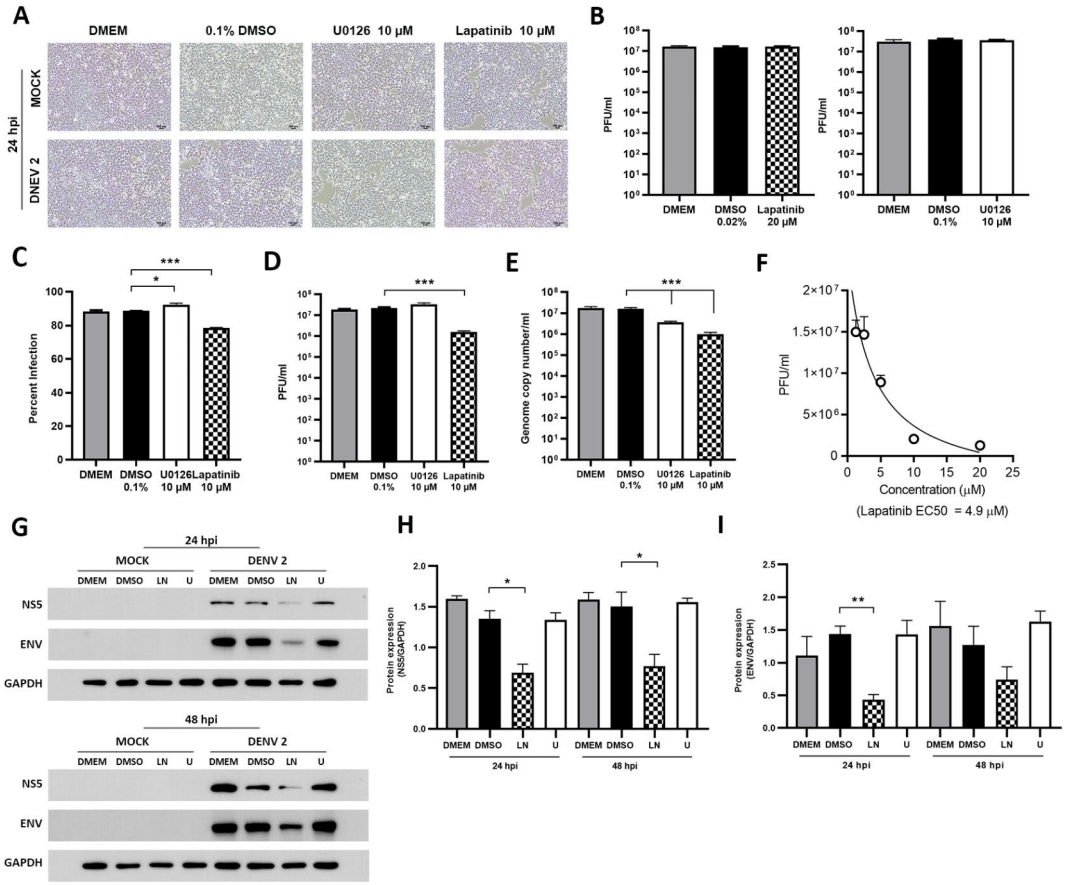

Fig. 3. Antiviral activity of lapatinib against DENV 2. Lapatinib and UO126 were used to treat HEK293T/17 cells after mock infection or infection with with DENV 2 MOI 5. Mock infected and infected cells were collected at 24 h post-infection as appropriate and investigated for (**A**) cell morphology (**B**) virucidal activity (**C**) percentage of infection (**D**) viral production (**E**) viral genome copy (**F**) EC_{50} (viral production) (**G**) viral protein expression at 24 and 48 h post-infection (**H**) quantitative of viral protein NS, and (**I**) ENV expression normalized against GAPDH. All experiments were conducted as independent triplicates, with duplicate plaque assay where appropriate. $^{*}P<0.05$, $^{**}P<0.01$, $^{***}P<0.001$. Composite images are shown (**G**) consisting of successive antibody probings of the same membrane which are separated by white bars. Full, uncropped western blots can be found in the supplemental materials.

with U0126 showed a slight increase in the percentage of infected cells (Fig. 3C), as well as a slight, but not statistically significant increase in virus titer (Fig. 3D). However, a reduction was seen in genome copy number (Fig. 3E), although the significance of this is unclear. To determine the EC_{50} of lapatinib, infected HEK293T/17 cells were treated with 1.25, 2.5, 5, 10, and 20 μM of lapatinib, and the virus production was determined at 24 h post-infection by standard plaque assay. The results showed that lapatinib can reduce viral production even in the lowest concentration 1.25 μM (Fig. 3F), and the calculated EC_{50} of lapatinib was 4.9 μM, giving a SI of 26.09. Moreover, lapatinib treatment reduced viral protein expression for both nonstructural (NS5) and structural (ENV) proteins (Fig. 3G-I).

Lapatinib affects the phosphorylation of Akt and ERK1/2 in the early state of threatening

Lapatinib acts indirectly to affect FASN activity via HER2 inhibition which affects the downstream pathways of Ras-Raf MEK-ERK1/2 and PI3K/Akt[37]. To investigate the effect on downstream signaling pathways upon DENV 2 infection in lapatinib treated cells, the phosphorylation of Akt and ERK1/2, representatives of both pathways was investigated by western blot analysis. HEK293T/17 cells were therefore infected with DENV 2 and then either untreated, or treated with lapatinib, U0126 or DMSO (compound diluent) and at 24 h post-infection proteins were collected and analyzed by western blot with phospho-Akt and phospho-ERK1/2 specific antibodies, as well as antibodies to total AKT and ERK1/2. The results (Fig. 4A, B) showed that infection significantly reduced phosphorylation of AKT (as seen in DMEM and DMSO controls), and while both lapatinib and U0126 reduced phosphorylation of AKT in infected cells as compared to mock, the reduction was not significant.

For ERK1/2 phosphorylation it was seen that ERK1/2 phosphorylation was significantly upregulated by DENV infection (Fig. 4A, C) as seen in DMEM and DMSO controls, laptanib treatment showed a

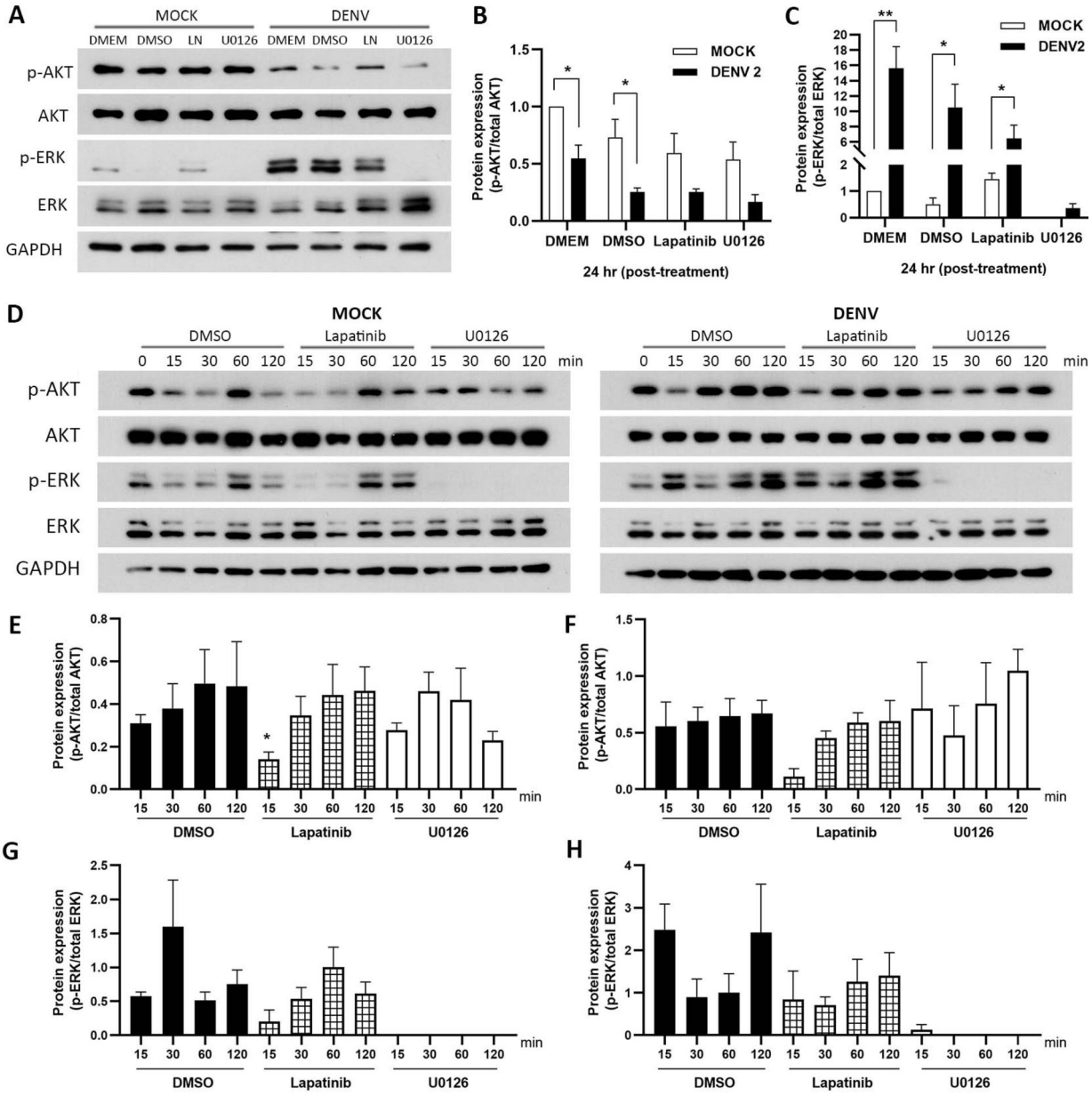

Fig. 4. Akt and ERK phosphorylation upon lapatinib treatment of DENV 2 infected HEK293T/17 cells. HEK297T/17 cells were infected with DENV 2 at MOI 5 and treated with lapatinib at 10 μM, U0126 at 10 μM, or 0.1% DMSO, or DMEM. After 24 h (**A**-**C**) the cell lysates were collected and analyzed by (**A**) western blot analysis after which signals were quantitated for (**B**) phospho-AKT/ total AKT and (**C**) phospho-ERK/ total ERK. In a subsequent experiment (**D**-**H**) HEK297T/17 cells were infected with DENV 2 at MOI 5 and treated with lapatinib at 10 μM, U0126 at 10 μM, or 0.1% DMSO, or DMEM. Cells were collected at 15, 30 60 and 120 min after treatment, lysates prepapred and again subjected to (**D**) western blot analysis after which signals were quantitated for (**E**-**F**) p-AKT/ total AKT and (**G**-**H**) phospho (P)-ERK/total ERK. All experiments were conducted as independent triplicates. $^{*}P < 0.05$, $^{**}P < 0.01$. Composite images are shown (**A**, **D**) consisting of successive antibody probings of the same membrane which are separated by white bars. Full, uncropped western blots can be found in the supplemental materials.

somewhat lower increase in ERK1/2 phosphorylation (as compared to the controls). Expectedly the MEK inhibitor U0126 completely inhibited ERK1/2 phosphorylation (Fig. 4A, C).

To investigate earlier time points, the experiment was repeated, but this time sample timepoints selected were 15, 30, 60, and 120 min after treatment with the compounds, and 0, 15, 30, 60, and 120 min for the DMSO control samples. The results (Fig. 4D-H) show that lapatinib significantly reduced AKT phosphorylation in mock infected cells at the earliest time point (15 min; Fig. 4D, E), the effect was short lived. Similarly, while lapatinib reduced phosphorylation of AKT in DENV infected cells at the

earliest time point examined (15 min), the results was not statistically significant (Fig. 4D, F). For ERK1/2 phosphorylation, no significant changes were seen with either infection (as compared to mock) nor treatment with lapatinib. However, U0126 completely eliminated ERK phosphorylation (Fig. 4D, G, H).

Lapatinib binding with NS5 of DENV 2 and ZIKV in an Silico model

Besides the indirect effect of lapatinib to inhibit the phosphorylation of FASN, lapatinib possibly has the potential to be a direct-acting-antiviral against NS5. NS5 is known as a conserved protein, and the priming loop is an indispensable structure as it is the initial site for RNA binding and synthesis (residues 785–810), and is a leading target for antiviral drug discovery efforts. The sequence homology in the priming loop site is around 76–81% and the binding site pocket of ZIKV (three glycine residues; G793, 801, 803) is larger and more flexible than of DENV (three bulkier amino acid residue; S791, A799, H801)[38]. Moreover, the area close to priming loop, the so-called "N-pocket" had been previously identified as a potential target binding site for small molecules[39]. Molecular docking of the target ligand, lapatinib, was performed to assess for possible interactions within the binding sites around the priming site close to N-pocket within the area of palm and thumb subdomain of ZIKV and DENV 2 NS5 proteins. Interestingly, lapatinib showed a lower binding energy with both ZIKV and DENV 2 as compared with the positive control, G80 (Table 1). Even though most of the active binding site around the N-pocket and the priming loop is conserved among orthoflaviviruses, the variation in other regions causes conformational changes in the binding pocket shape, resulting in different binding energy among viruses, and affecting the interactions between the amino acids, and the ligand at the binding site. Lapatinib fit more into the NS5 of ZIKV than DENV 2 (Fig. 5A,B), probably due to a more narrow binding pocket. The primary intermolecular interaction of ZIKV NS5 was driven by three main hydrogen bonds at amino acid residues Ser798, Arg739, and Cys711, while in contrast, binding to DENV 2 NS5 was driven by one hydrogen bond at amino acid residue Arg737. Moreover, other intermolecular forces were involved in both ZIKV and DENV 2, for instance, alkyl and sulfur bonds (Fig. 5C, D).

Lapatinib has antiviral activity against ZIKV

According to molecular docking prediction results, lapatinib can bind directly to NS5 of ZIKV with a lower binding energy than DENV 2, suggesting it might have a greater antiviral activity towards ZIKV than DENV. Any possible direct virucidal activity of lapatinib or U0126 towards ZIKV was assessed by incubating lapatinib or U0126 with stock virus for 1 h, and then assessing the remaining virus titer. The results showed that neither lapatinib nor U0126 had a direct virucidal activity to ZIKV (Fig. 6A). Concentrations of lapatinib lower than 25 μM showed no sign of cell toxicity with regards to morphological changes, and the CC_{50} of lapatinib was 75.83 μM (Supplemental Fig. 5A, B). The morphology of the A549 cells infected with ZIKV at 24 h post-infection was not changed when the cells were treated with 10 μM of both compounds (Fig. 6B, upper panel). To assess possible antiviral activity of lapatinib, A549 cells were infected with ZIKV at MOI 1 and then treated with lapatinib or U0126. At 24–48 h post-infection, cells and supernatant were collected to determine the percentage of viral infection, viral production as well as viral genome copy number. The morphology of A549 cells was changed as a consequence of ZIKV infection at 48 h post-infection in all treated or non-treated conditions. Approximately half of the A549 cells were detached, shrunk, and dead (Fig. 6B, lower panel). Lapatinib significantly reduced ZIKV infection in the cell (Fig. 6C), viral production (Fig. 6D), and viral genome copy number (Fig. 6E). Interestingly, the infectious titer of the virus was reduced by some $3Log_{10}$, while the genome copy number was reduced by some $2Log_{10}$, suggesting that lapatinib affects not only the overall replication, but also the fidelity of replication. Protein expression of NS5 and ZIKV E protein was evaluated at 24 and 48 h by western blotting (Fig. 6F) and quantification of the signal (Fig. 6G, H) showed that expression of NS5 was significantly reduced at 24 h post infection, and reduced but not significanly at 48 h post-infection, while ZIKV E protein was reduced, but not significantly at 24 h.p.i, and was significantly reduced at 48 h.p.i.

To determine the effective concentration of lapatinib, A549 cells were again infected with ZIKV, and were then treated with different concentrations of lapatinib, and virus titer was determined at 24 post-infection. The results (Fig. 6I) showed a dose dependent reduction in titer, and the calculated EC_{50} for lapatinib towards ZIKV was was 2 μM and the calculated SI was 37.92.

To provide additional assurance on the antiviral activity of lapatinib towards ZIKV, a second ZIKV strain (MU1-2017), which was isolated from tissues from the autopsy of a fetus medically terminated for reasons of congenital Zika syndrome32 was used to infect A549 cells at MOI of 1. Post-infection cells were treated with lapatinib and the percentage of infection and viral production were determined at 24 h post-infection. The results (Fig. 7) showed that lapatinib could reduce both the percentage of infection and viral production. Again, the reduction of viral titer was on the order of 3Log10.

A549 cells were infected with ZIKV strain MU1 at MOI 1 and after 24 h (A) the percentage infection was determined by flow cytometry and (B) the infectios titer in the supernatant was determined by plaque assay. All experiments were undertaken as independent biological triplicates with duplicate plaque assay where appropriate. $^{**}P < 0.01$, $^{***}P < 0.001$.

Compounds	Binding energy (kcal/mol)	
	ZIKV	DENV 2
Lapatinib	−9.5	−8.6
G80	−6.5	−6.6

Table 1. The binding energy of lapatinib and G80 to NS5 of ZIKV and DENV.

Discussion

The human pathogenic viruses in the genus *Orthoflavivirus* are primarily transmitted to humans by hematophagous arthropods such as ticks and mosquitoes[40]. In tropical and sub-tropical countries around the world, the primary concern is those viruses that are transmitted by mosquitoes, which can impose a heavy health burden, especially in poorer countries. DENV became a serious population threat after the second world war, where the circulation of multiple DENV serotypes and rapid urbanization in Southeast Asia prompted the emergence of the more serious hemorrhagic form of the disease[41]. Despite nearly 80 years of research, there remains no specific treatment, and as yet no widely available vaccine. In contrast thelong established presence of DENV in many countries around the world, ZIKV emerged suddenly starting from the outbreak of Zika fever in French Polynesia in 2013[9]. Within a very short period of time the Asian lineage ZIKV spread around the globe[42]. As with DENV there is no specific treatment, and no vaccine is available. With around 27 human pathogenic mosquito tranmsmitted viruses in the genus *Orthoflavivirus*[43], it would be desirable to find drugs that are able to exert an antiviral effect on all of the viruses in the genus. While direct targeting of the virus can be beneficial in terms of lower toxicity, the Orthoflaviviral RNA-dependent RNA polymerase (NS5) has no proofreading activity, leading to a high variation rate that can quickly overcome the effectiveness of the drug[44]. In contrast, targeting drugs to host cell proteins is likely to result in a broader spectrum of action and lower levels of drug resistance.

However, *de novo* drug development is a long and expensive process since most drugs do not pass clinical trials[45]. Drug repurposing overcomes much of this issue as the drugs have safe profiles in application to other diseases.

Our previous study showed that lipid metabolism is altered during DENV infection, and that inhibition of FASN by siRNA or orlistat significantly reduced viral production[23]. Other studies have also shown the impact of FASN inhibitors on viral replication. For example celulinin and C75 whose major target is the KS domain of FASN reduced DENV infectious particles in infected Huh-7.5 cells by approximately 1 and 2 log, respectively[27]. Triclosan, an inhibitor acting on the inhibition of the ER domain of FASN affected viral production albeit to a lesser extent than the well-known FASN inhibitor, orlistat, which acts upon the thioesterase domain. Even though the $EC_{50}$of both compounds is not very different, the SI of triclosan is about 3–4 fold times lower at 3.99 as compared to the SI of 13.13 for orlistat[23].

In addition to acting on the thioesterase domain of FASN, studies have shown that orlistat can act on other proteins that can affect viral replication. A proteomic analysis identified pyruvate kinase M2 (PKM2) as down-regulated in ovarian cancer cells treated with orlistat[46]. Phosphorylation of PKM2 has been studied in response to DENV infection in U937 cells, and inhibition of PKM2 reduced DENV production[47]. Furthermore, a proteomic analysis of the effects of orlistat identified seven target proteins besides FASN including GAPDH, β-tubulin, RPL7a, RPL14, RPS9, Annexin A2, and HSPAB1[48]. Several of these proteins have been linked to roles in DENV replication, for instance, GAPDH has been shown to interact with NS3 of DENV resulting in reduced glycolytic activity. Another study showed that GAPDH was down-regulated in DENV infected liver (Hep3B) cells, resulting in reduced glycolysis[49]. Both beta- and alpha-tubulin have been shown to be involved in the binding of DENV to C6/36 cells[50]. A further study showed that the ribosome subunits RPL7 and RPL14 interacted with DENV NS5[51]. Lastly, annexin A2 is required for the binding of DENV to Vero cells[52]. Therefore, orlistat could have effects on several mechanisms, in addition to the inhibition of FASN. Interestingly, the reduction of the percentage infection in cells treated with triclosan or orlistat was approximately 13% and 26% as compared to untreated cells, respectively. However the reduction in viral production and genome copy number was 48%, and 63%, for triclosan, and 75% and 68% for orlistat. This implies that these compounds both may be affecting other processes such as virion assembly or release resulting in the envelope protein accumulating in the cells but resulting in significantly greater reductions of virions in the supernatant. Additionally we note that while triclosan reduced FASN expression, no significant effects were seen on NS5 and E protein expression as determined by western blotting. However analysis of level of infection by flow cytometry (which detects E protein) showed some reduction in the level of infection. It is currently unclear whether this reflects technical sensitivity issues, or there is an additional undelying cause of the apparent discrepancy.

Besides the direct inhibitor of FASN, triclosan, we investigated a potential inhibitor that has an indirect effect on FASN, namely lapatinib. Lapatinib works by two mechanisms, a direct reduction of HER2 itself and a reduction of downstream phosphorylation which includes the phosphorylation of FASN[53,54]. In this study we showed that lapatinib has antiviral activity against both ZIKV and DENV, which is similar

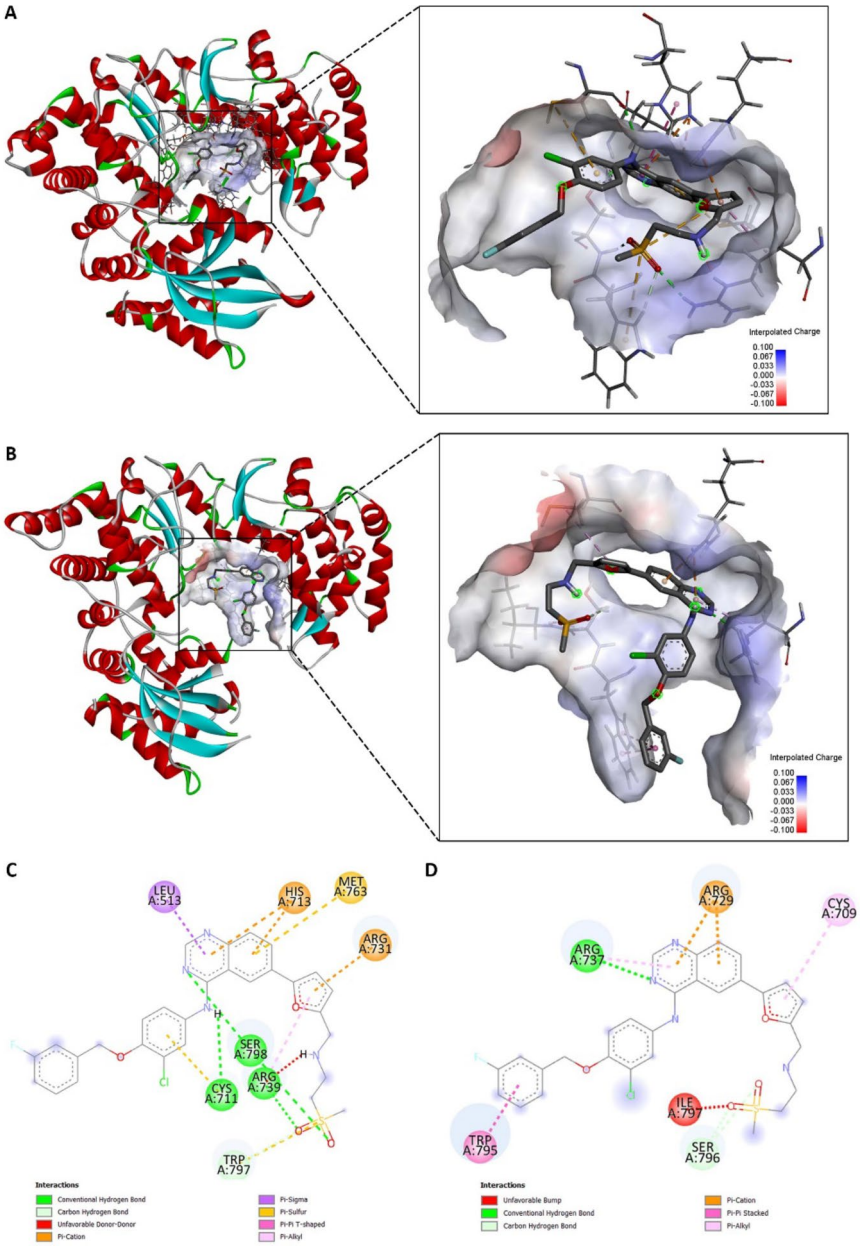

Fig. 5. Molecular docking of lapatinib with NS5 proteins of ZIKV and DENV 2. NS5 of ZIKV and DENV 2, -PDB ID #:6LD3 and 5K5M were docked and visualized by AutoDock Vina (version 1.1.2, https://vina.scripps.edu/) in the same position at the priming loop site. The docking of (**A**) ZIKV and (**B**) DENV 2 NS5 with the ligand (lapatinib) and other binding sites involved aare shown in as ribbon structures, with the interpolative charge ranging from −0.1–0.1. The 2-dimensional structures show the binding site of lapatinib with NS5 of (**C**) ZIKV and (**D**) DENV, with the different amino acid binding sites and forces.

to the new synthetic compound, L3 which decreases endogenous HER2 and inhibits phosphorylation of downstream proteins[53]. However, lapatinib may be beneficial over L3, as lapatinib is an approved drug[55].

Moreover, lapatinib has a potential direct-acting antiviral effect through NS5 of both DENV and ZIKV which showed a good binding affinity in molecular docking. Our study found that the binding energy of lapatinib to ZIKV is lower than DENV via molecular docking corresponding to the in vitro experiments which showed a greater effect of lapatinib against ZIKV than against DENV.

The activity of inhibitors to the N-pocket close to the priming loop of DENV serotype 3 can also inhibit ZIKV in the N-pocket area, and reduced ZIKV replication in vitro with an EC_{50} = 24.3 μM[56]. In our study lapatinib bound to the N-pocket of both ZIKV and DENV NS5 with different affinities. For ZIKV, lapatinib shared the common six binding molecules including Leu513, His713, Met763, Ser798, Cys711, and Arg739 with the ligands Cpd15 while DENV has 4 positions including Arg729, Arg737, and Cys709

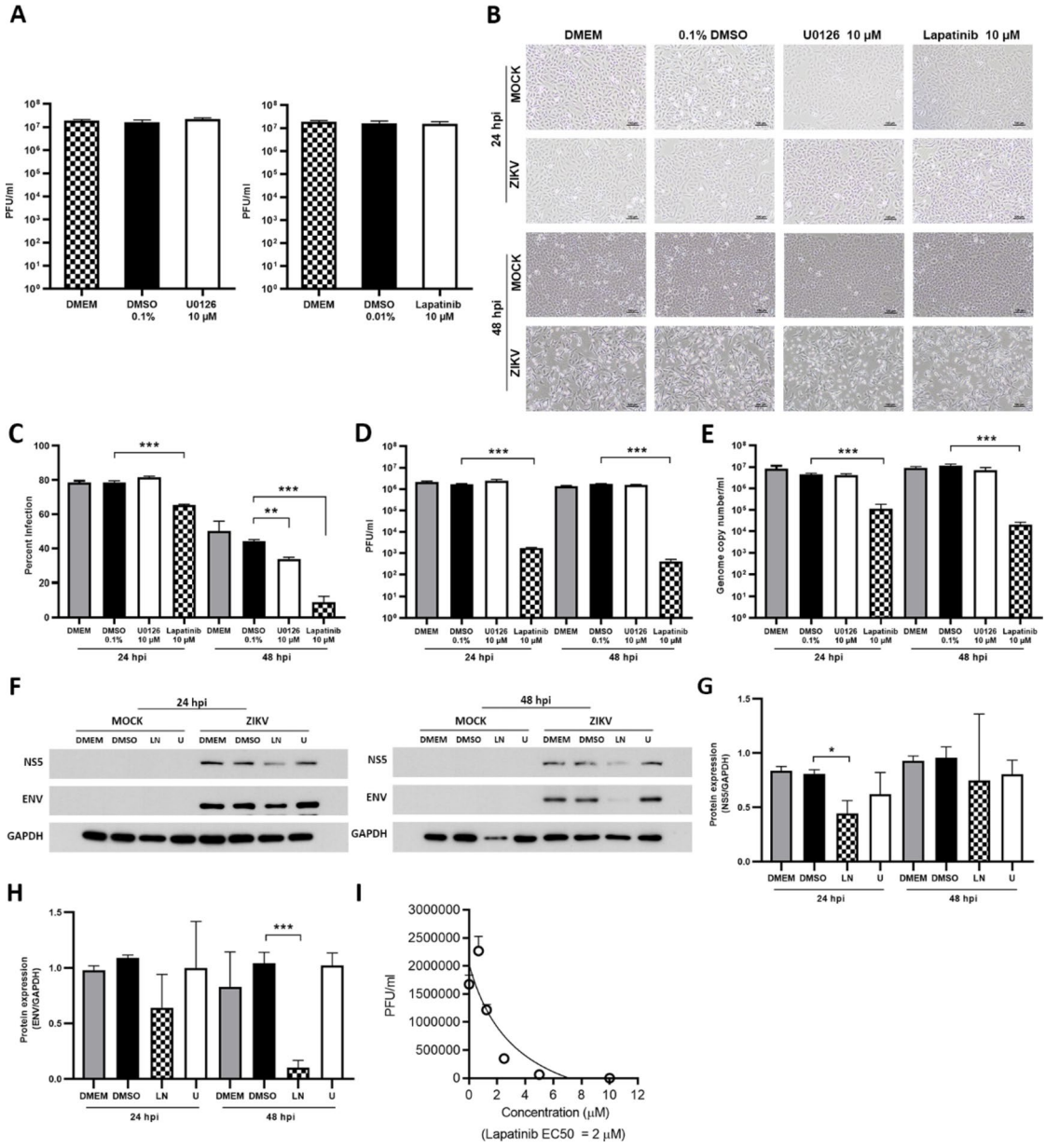

Fig. 6. Possible direct virucidal activity of U1026 or lapatinib towards ZIKV was established by incubating stock virus with each compound with DMEM being used as a negative control, after which the remaining virus titer was established by plaque assay. Subsequently, ZIKV infected A549 cells (MOI 1) were treated with 10 μM lapatinib, 10 μM UO126, DMEM or 0.1% DMSO and were cultured for 24–48 h and subsequently cells and supernatant were collected and (**B**) cell morphology was examined by light microscopy, (**C**) the percentage infection determined by flow cytometry, (**D**) the virus titer determined by plaque assay, (**E**) the genome copy number determined by real-time quantitative PCR, and (**F**) the expression of ZIKV E and NS5 proteins determined by western blot analysis and signal intensity was quantitated (**G**, **H**). Subsequently, (**I**) ZIKV infected A549 cells (MOI 1) were treated with differing concentrations of lapatinib (0.675 μM to 10 μM) for 24 h after which the virus titer was determined by plaque assay. All experiments were conducted as independent triplicates, with duplicate plaque assay where appropriate. $^{*}P<0.05$, $^{**}P<0.01$, $^{***}P<0.001$. Composite images are shown (**F**) consisting of successive antibody probings of the same membrane which are separated by white bars. Full, uncropped western blots can be found in the supplemental materials.

with the ligand NITD29. Due to the conservation of the priming loop and N-pocket inhibitors which targeted this area could be possibly have functions as broad spectrum antivirals to other Orthoflaviviruses.

Again, there was some discordance in the magnitude of the effect when comparing different markers, with the infectious virus production being decreased by some $3Log_{10}$, while the viral genome copy number in the supernatant showed about a 2Log10 reduction. This would be consistent with a reduced fidelity of replication generating more non-functional genomes.

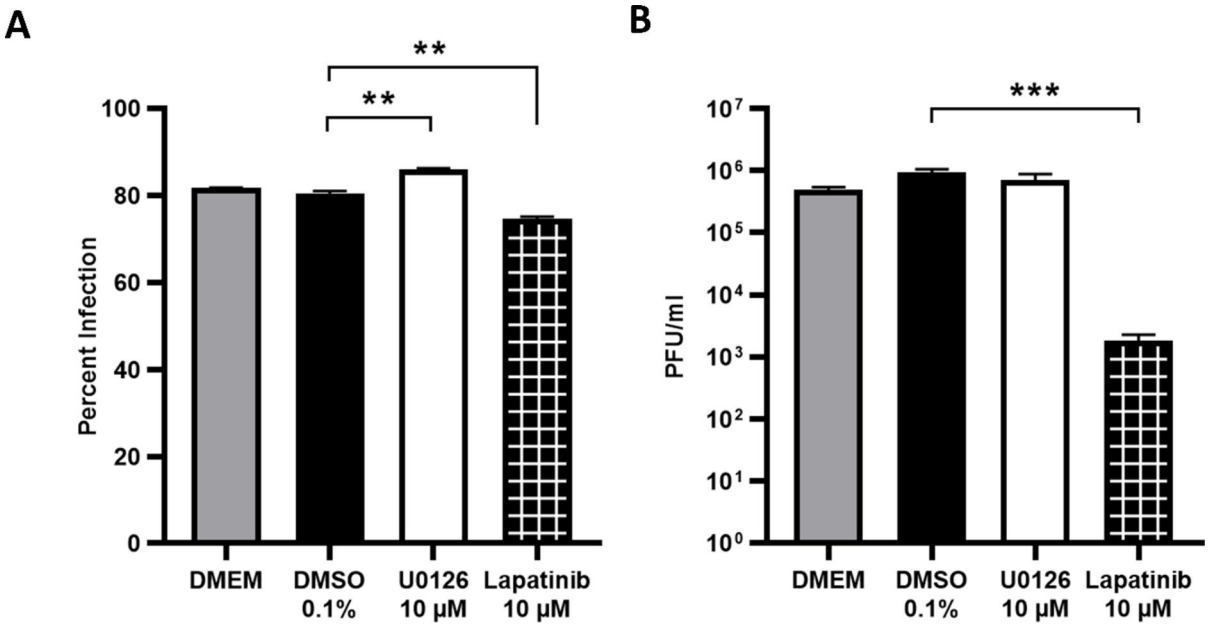

Fig. 7. Antiviral activity of lapatinib against ZIKV strain MU1-2017 infected A549 cells.

In our experiment, we found that lapatinib acted rapidly on a downstream phosphorylation target of HER2 which is phospho-Akt. This result corresponds to a previous study which showed that phospho-Akt responded to the virus infection after 5 min post-infection, and gradually increased until 1 h post-infection before dropping after 12 h post-infection[57]. In this aspect, DENV-induced phospho-Akt acts as an anti-apoptotic to prolong the virus infection[57]. In our study DENV infection resulted in the strong phosphorylation of ERK in HEK293T/17 cells, which was completely abolished by the ERK inhibitor U0126. A previous study showed that U0126 decreased the viral production in JEV and DENV-infected cells[58]. In our study, even though the inhibitor U0126 had a long lasting inhibition of the phosphorylation of ERK, this had no effect on viral infection and production. Our result is consistent with other studies that have shown that azathioprine which inhibits Vav signaling resulting in the reduction of ERK phosphorylation did not affect DENV production[59]. Similarly, inhibition of ERK phosphorylation was shown to protect DENV infected hepatocytes from apoptosis, but no effect was seen on viral production[60]. The superior inhibitory effect of lapatinib on viral replication as compared to U0126 likely arises from the potential dual mechanism of action of laptanib, which acts through inhibition of signal transduction, as well as a possible effect directly as an NS5 inhibitor. Future studies will need to examine in greater detail the mechanism of action laptanib, particularly as to whether one mechanism predominates, or both act in combination or even possibly synergistically.

Some studies have shown that triclosan might have long-term adverse effects on cells[61]. The EC_{50} of triclosan is 10.21, however, a concentration of the drug more than 10 μM is toxic to cells. This means that triclosan cannot reduce DENV by more than 50% due to the toxicity of triclosan at high concentrations. Moreover, triclosan contains two benzine rings, which make triclosan more insoluble in water, subsequently affecting the absorption of the compound to target cells. Thus, while triclosan is useful in understanding how FASN modulates viral infection, it has poor characteristics for development as a therapeutic tool.

Lapatinib is an approved drug for the treatment of breast cancer, but the cost of the drug is high[62]. Another concern is toxicity to normal cells at higher concentrations. However, while lapatinib has useful activity against DENV, lapatinib is highly effective against ZIKV with an $EC_{50}$of 2 μM and an SI of 37.92, which suggests that lapatinib might have some application in the treatment of selected cases. CZS is more likely to occur when pregnant women are infected with ZIKV in the first or second trimester of their pregnancy but CZS can also occur when infection occurs in the third trimester[63], however chemotherapy is administered to pregnant women only after the first trimester[64]. Thus there is a window for possible application of lapatinib therapeutically. However, a better alternative would be the development of compounds with the same structural features of lapatinib, but without the associated cytotoxicity.

Data availability

"All data generated or analyzed during this study are included in this published article (and its Supplementary Information file). NCBI accession numbers for the sequences of viruses used in this study are DENV 2 (NCBI Accession number NC_001474), ZIKV SV0010/15 (NCBI accession number KX051562) and MU1-2017 (identical to NCBI accession number MF996804)."

Received: 23 November 2024; Accepted: 20 March 2025
Published online: 28 March 2025

References

1. Postler, T. S. et al. Renaming of the genus flavivirus to orthoflavivirus and extension of binomial species names within the family flaviviridae. *Arch. Virol.* **168**, 224. https://doi.org/10.1007/s00705-023-05835-1 (2023).
2. Bhatt, S. et al. The global distribution and burden of dengue. *Nature* **496**, 504–507. https://doi.org/10.1038/nature12060 (2013).
3. Gubler, D. J. Dengue and dengue hemorrhagic fever. *Clin. Microbiol. Rev.* **11**, 480–496. https://doi.org/10.1128/CMR.11.3.480 (1998).
4. Imrie, A. et al. Antibody to dengue 1 detected more than 60 years after infection. *Viral Immunol.* **20**, 672–675. https://doi.org/10.1089/vim.2007.0050 (2007).
5. Halstead, S. B., Porterfield, J. S. & O'Rourke, E. J. Enhancement of dengue virus infection in monocytes by flavivirus antisera. *Am. J. Trop. Med. Hyg.* **29**, 638–642. https://doi.org/10.4269/ajtmh.1980.29.638 (1980).
6. Guo, C. et al. Global epidemiology of dengue outbreaks in 1990–2015: A systematic review and Meta-Analysis. *Front. Cell. Infect. Microbiol.* **7**, 317. https://doi.org/10.3389/fcimb.2017.00317 (2017).
7. Wang, L. et al. From mosquitos to humans: genetic evolution of Zika virus. *Cell. Host Microbe.* **19**, 561–565. https://doi.org/10.1016/j.chom.2016.04.006 (2016).
8. Shen, S. et al. Phylogenetic analysis revealed the central roles of two African countries in the evolution and worldwide spread of Zika virus. *Virol. Sin.* **31**, 118–130. https://doi.org/10.1007/s12250-016-3774-9 (2016).
9. Cao-Lormeau, V. M. et al. Zika virus, French Polynesia, South Pacific, 2013. *Emerg. Infect. Dis.* **20**, 1085–1086. https://doi.org/10.3201/eid2006.140138 (2014).
10. Campos, G. S., Bandeira, A. C. & Sardi, S. I. Zika virus outbreak, Bahia, Brazil. *Emerg. Infect. Dis.* **21**, 1885–1886. https://doi.org/10.3201/eid2110.150847 (2015).
11. Paixao, E. S., Barreto, F., Teixeira Mda, G., Costa Mda, C. & Rodrigues, L. C. History, epidemiology, and clinical manifestations of Zika: A systematic review. *Am. J. Public. Health.* **106**, 606–612. https://doi.org/10.2105/AJPH.2016.303112 (2016).
12. Brasil, P. et al. Guillain-Barre syndrome associated with Zika virus infection. *Lancet* **387**, 1482. https://doi.org/10.1016/S0140-6736(16)30058-7 (2016).
13. Moore, C. A. et al. Characterizing the pattern of anomalies in congenital Zika syndrome for pediatric clinicians. *JAMA Pediatr.* **171**, 288–295. https://doi.org/10.1001/jamapediatrics.2016.3982 (2017).
14. Tan, Z. et al. ZIKV infection activates the IRE1-XBP1 and ATF6 pathways of unfolded protein response in neural cells. *J. Neuroinflammation.* **15**, 275. https://doi.org/10.1186/s12974-018-1311-5 (2018).
15. Thepparit, C. et al. Dengue 2 infection of HepG2 liver cells results in Endoplasmic reticulum stress and induction of multiple pathways of cell death. *BMC Res. Notes.* **6**, 372. https://doi.org/10.1186/1756-0500-6-372 (2013).
16. Panyasrivanit, M., Khakpoor, A., Wikan, N. & Smith, D. R. Co-localization of constituents of the dengue virus translation and replication machinery with amphisomes. *J. Gen. Virol.* **90**, 448–456. https://doi.org/10.1099/vir.0.005355-0 (2009).
17. Stoyanova, G. et al. Zika virus triggers autophagy to exploit host lipid metabolism and drive viral replication. *Cell. Commun. Signal.* **21**, 114. https://doi.org/10.1186/s12964-022-01026-8 (2023).
18. Hitakarun, A. et al. Cell type variability in the incorporation of lipids in the dengue virus virion. *Viruses* **14** https://doi.org/10.3390/v14112566 (2022).
19. Leier, H. C. et al. A global lipid map defines a network essential for Zika virus replication. *Nat. Commun.* **11**, 3652. https://doi.org/10.1038/s41467-020-17433-9 (2020).
20. Martín-Acebes, M. A., Vázquez-Calvo, Á. & Saiz, J. C. Lipids and flaviviruses, present and future perspectives for the control of dengue, Zika, and West nile viruses. *Prog Lipid Res.* **64**, 123–137. https://doi.org/10.1016/j.plipres.2016.09.005 (2016).
21. Wakil, S. J. Fatty acid synthase, a proficient multifunctional enzyme. *Biochemistry* **28**, 4523–4530. https://doi.org/10.1021/bi00437a001 (1989).
22. Asturias, F. J. et al. Structure and molecular organization of mammalian fatty acid synthase. *Nat. Struct. Mol. Biol.* **12**, 225–232. https://doi.org/10.1038/nsmb899 (2005).
23. Tongluan, N. et al. Involvement of fatty acid synthase in dengue virus infection. *Virol. J.* **14**, 28. https://doi.org/10.1186/s12985-017-0685-9 (2017).
24. Hitakarun, A. et al. Evaluation of the antiviral activity of Orlistat (tetrahydrolipstatin) against dengue virus, Japanese encephalitis virus, Zika virus and Chikungunya virus. *Sci. Rep.* **10**, 1499. https://doi.org/10.1038/s41598-020-58468-8 (2020).
25. Chen, Q. et al. Metabolic reprogramming by Zika virus provokes inflammation in human placenta. *Nat. Commun.* **11**, 2967. https://doi.org/10.1038/s41467-020-16754-z (2020).
26. Martín-Acebes, M. A., Blázquez, A. B., Jiménez de Oya, N., Escribano-Romero, E. & Saiz, J. C. West nile virus replication requires fatty acid synthesis but is independent on phosphatidylinositol-4-phosphate lipids. *PLoS One.* **6**, e24970. https://doi.org/10.1371/journal.pone.0024970 (2011).
27. Heaton, N. S. et al. Dengue virus nonstructural protein 3 redistributes fatty acid synthase to sites of viral replication and increases cellular fatty acid synthesis. *Proc. Natl. Acad. Sci. U S A.* **107**, 17345–17350. https://doi.org/10.1073/pnas.1010811107 (2010).
28. Zhang, J. S. et al. Natural fatty acid synthase inhibitors as potent therapeutic agents for cancers: A review. *Pharm. Biol.* **54**, 1919–1925. https://doi.org/10.3109/13880209.2015.1113995 (2016).
29. Liu, B., Wang, Y., Fillgrove, K. L. & Anderson, V. E. Triclosan inhibits enoyl-reductase of type I fatty acid synthase in vitro and is cytotoxic to MCF-7 and SKBr-3 breast cancer cells. *Cancer Chemother. Pharmacol.* **49**, 187–193. https://doi.org/10.1007/s00280-001-0399-x (2002).
30. Jin, Q. et al. Fatty acid synthase phosphorylation: a novel therapeutic target in HER2-overexpressing breast cancer cells. *Breast Cancer Res.* **12**, R96. https://doi.org/10.1186/bcr2777 (2010).
31. Nakabayashi, H., Taketa, K., Miyano, K., Yamane, T. & Sato, J. Growth of human hepatoma cells lines with differentiated functions in chemically defined medium. *Cancer Res.* **42**, 3858–3863 (1982).
32. Jitsatja, A. et al. Comparative analysis of a Thai congenital-Zika-syndrome-associated virus with a Thai Zika-fever-associated virus. *Arch. Virol.* **165**, 1791–1801. https://doi.org/10.1007/s00705-020-04667-7 (2020).
33. Sawadpongpan, S. et al. Investigation of the activity of Baicalein towards Zika virus. *BMC Complement. Med. Ther.* **23**, 143. https://doi.org/10.1186/s12906-023-03971-4 (2023).
34. Henchal, E. A., Gentry, M. K., McCown, J. M. & Brandt, W. E. Dengue virus-specific and flavivirus group determinants identified with monoclonal antibodies by indirect Immunofluorescence. *Am. J. Trop. Med. Hyg.* **31**, 830–836. https://doi.org/10.4269/ajtmh.1982.31.830 (1982).
35. Berman, H., Henrick, K. & Nakamura, H. Announcing the worldwide protein data bank. *Nat. Struct. Biol.* **10**, 980. https://doi.org/10.1038/nsb1203-980 (2003).
36. Berman, H. M. et al. The protein data bank. *Nucleic Acids Res.* **28**, 235–242. https://doi.org/10.1093/nar/28.1.235 (2000).
37. Medina, P. J. & Goodin, S. Lapatinib: a dual inhibitor of human epidermal growth factor receptor tyrosine kinases. *Clin. Ther.* **30**, 1426–1447. https://doi.org/10.1016/j.clinthera.2008.08.008 (2008).
38. Godoy, A. S. et al. Crystal structure of Zika virus NS5 RNA-dependent RNA polymerase. *Nat. Commun.* **8**, 14764. https://doi.org/10.1038/ncomms14764 (2017).

39. Lim, S. P. et al. Potent allosteric dengue virus NS5 polymerase inhibitors: mechanism of action and resistance profiling. *PLoS Pathog.* **12**, e1005737. https://doi.org/10.1371/journal.ppat.1005737 (2016).
40. Gould, E. A. & Solomon, T. Pathogenic flaviviruses. *Lancet* **371**, 500–509. https://doi.org/10.1016/S0140-6736(08)60238-X (2008).
41. Gubler, D. J. Dengue/dengue haemorrhagic fever: history and current status. *Novartis Found. Symp.* **277**, 3–16. https://doi.org/10.1002/0470058005.ch2 (2006). discussion 16–22, 71 – 13.
42. Wikan, N. & Smith, D. R. Zika virus: history of a newly emerging arbovirus. *Lancet Infect. Dis.* **16**, e119–e126. https://doi.org/10.1016/S1473-3099(16)30010-X (2016).
43. Smith, D. R. Waiting in the wings: the potential of mosquito transmitted flaviviruses to emerge. *Crit. Rev. Microbiol.* **43**, 405–422. https://doi.org/10.1080/1040841X.2016.1230974 (2017).
44. Venkataraman, S., Prasad, B. & Selvarajan, R. RNA dependent RNA polymerases: insights from structure, function and evolution. *Viruses* **10** https://doi.org/10.3390/v10020076 (2018).
45. Wouters, O. J., McKee, M. & Luyten, J. Estimated research and development investment needed to bring a new medicine to market, 2009–2018. *JAMA* **323**, 844–853. https://doi.org/10.1001/jama.2020.1166 (2020).
46. Huang, H. Q. et al. Orlistat, a novel potent antitumor agent for ovarian cancer: proteomic analysis of ovarian cancer cells treated with Orlistat. *Int. J. Oncol.* **41**, 523–532. https://doi.org/10.3892/ijo.2012.1465 (2012).
47. Wongtrakul, J. et al. Phosphoproteomic analysis of dengue virus infected U937 cells and identification of pyruvate kinase M2 as a differentially phosphorylated phosphoprotein. *Sci. Rep.* **10**, 14493. https://doi.org/10.1038/s41598-020-71407-x (2020).
48. Yang, P. Y. et al. Activity-based proteome profiling of potential cellular targets of Orlistat–an FDA-approved drug with anti-tumor activities. *J. Am. Chem. Soc.* **132**, 656–666. https://doi.org/10.1021/ja907716f (2010).
49. Chumchanchira, C. et al. Glycolysis is reduced in dengue virus 2 infected liver cells. *Sci. Rep.* **14**, 8355. https://doi.org/10.1038/s41598-024-58834-w (2024).
50. Chee, H. Y. & AbuBakar, S. Identification of a 48 kda tubulin or tubulin-like C6/36 mosquito cells protein that binds dengue virus 2 using mass spectrometry. *Biochem. Biophys. Res. Commun.* **320**, 11–17. https://doi.org/10.1016/j.bbrc.2004.05.124 (2004).
51. Poyomtip, T. et al. Development of viable TAP-tagged dengue virus for investigation of host-virus interactions in viral replication. *J. Gen. Virol.* **97**, 646–658. https://doi.org/10.1099/jgv.0.000371 (2016).
52. Aliyu, I. A., Ling, K. H., Hashim, M., Lam, N. F., Chee, H. & J. Y. & Y. Annexin II as a dengue virus serotype 2 interacting protein mediating virus interaction on Vero cells. *Viruses* **11** https://doi.org/10.3390/v11040335 (2019).
53. Chuang, F. K. et al. Antiviral activity of compound L3 against dengue and Zika viruses in vitro and in vivo. *Int. J. Mol. Sci.* **21** https://doi.org/10.3390/ijms21114050 (2020).
54. Vazquez-Martin, A., Colomer, R., Brunet, J., Lupu, R. & Menendez, J. A. Overexpression of fatty acid synthase gene activates HER1/HER2 tyrosine kinase receptors in human breast epithelial cells. *Cell. Prolif.* **41**, 59–85. https://doi.org/10.1111/j.1365-2184.2007.00498.x (2008).
55. Ryan, Q. et al. FDA drug approval summary: lapatinib in combination with capecitabine for previously treated metastatic breast cancer that overexpresses HER-2. *Oncologist* **13**, 1114–1119. https://doi.org/10.1634/theoncologist.2008-0816 (2008).
56. Gharbi-Ayachi, A. et al. Non-nucleoside inhibitors of Zika virus RNA-Dependent RNA polymerase. *J. Virol.* **94** https://doi.org/10.1128/JVI.00794-20 (2020).
57. Lee, C. J., Liao, C. L. & Lin, Y. L. Flavivirus activates phosphatidylinositol 3-kinase signaling to block caspase-dependent apoptotic cell death at the early stage of virus infection. *J. Virol.* **79**, 8388–8399. https://doi.org/10.1128/jvi.79.13.8388-8399.2005 (2005).
58. Albarnaz, J. D. et al. MEK/ERK activation plays a decisive role in yellow fever virus replication: implication as an antiviral therapeutic target. *Antiviral Res.* **111**, 82–92. https://doi.org/10.1016/j.antiviral.2014.09.004 (2014).
59. Cowell, E. et al. Vav proteins do not influence dengue virus replication but are associated with induction of phospho-ERK, IL-6, and Viperin mRNA following DENV infection in vitro. *Microbiol. Spectr.* **12**, e0239123. https://doi.org/10.1128/spectrum.02391-23 (2024).
60. Sreekanth, G. P. et al. Role of ERK1/2 signaling in dengue virus-induced liver injury. *Virus Res.* **188**, 15–26. https://doi.org/10.1016/j.virusres.2014.03.025 (2014).
61. Chen, X., Mou, L., Qu, J., Wu, L. & Liu, C. Adverse effects of triclosan exposure on health and potential molecular mechanisms. *Sci. Total Environ.* **879**, 163068. https://doi.org/10.1016/j.scitotenv.2023.163068 (2023).
62. Roskoski, R. Jr. Cost in the united States of FDA-approved small molecule protein kinase inhibitors used in the treatment of neoplastic and non-neoplastic diseases. *Pharmacol. Res.* **199**, 107036. https://doi.org/10.1016/j.phrs.2023.107036 (2024).
63. Brasil, P. et al. Zika virus infection in pregnant women in Rio de Janeiro. *N Engl. J. Med.* **375**, 2321–2334. https://doi.org/10.1056/NEJMoa1602412 (2016).
64. Wolters, V. et al. Management of pregnancy in women with cancer. *Int. J. Gynecol. Cancer.* **31**, 314–322. https://doi.org/10.1136/ijgc-2020-001776 (2021).

Acknowledgements

This work was supported by grants from Mahidol University (Fundamental Fund: fiscal year 2023 by National Science Research and Innovation Fund (NSRF)) and the National Research Council of Thailand (NRCT) and Mahidol University (NRCT5-RSA63015-03). S.S. was supported by a Royal Golden Jubilee Ph.D. scholarship from the National Research Council of Thailand (NRCT5- RGJ63012-139).

Author contributions

S. S. Roles: Investigation, Formal analysis, Vizualization, Writing – original draft, Writing – review & editingJ. J. Roles: Investigation, Writing – review & editingC. C. Roles: Investigation, Writing – review & editingD.R.S. Roles: Conceptualization, Supervision, Funding acquisition, Writing – original draft, Writing – review & editing.

Declarations

Competing interests

The authors declare no competing interests.

Additional information

Supplementary Information The online version contains supplementary material available at https://doi.org/10.1038/s41598-025-95346-7.

Correspondence and requests for materials should be addressed to D.R.S.